Electronic Supplementary Information for

Solvent-free carbothermal synthesis of 2D biochar stabilized nanoscale zerovalent iron composite for the oxidative degradation of organic pollutant

Xiao-Hu Dai[a,b], Hao-Xiang Fan[a], Chun-Yan Yi[c], Bing Dong[a,b], Shi-Jie Yuan[a,b]*

[a] State Key Laboratory of Pollution Control and Resource Reuse, College of Environmental Science and Engineering, Tongji University, Shanghai, 200092, China

[b] Shanghai Institute of Pollution Control and Ecological Security, Shanghai, 200092, China

[c] Shanghai Institutes for Biological Sciences, Chinese Academy of Sciences, Shanghai, 200031, China

***Corresponding author:**

Dr. Shi-Jie Yuan, Phone: +86-21-65986297; Fax: +86-21-65983602; E-mail: ysj@tongji.edu.cn

Scheme s1. Schematic illustration of the procedure used to construct the nZVI/biochar OCF-850.

Table s1. Comparison of the synthesis catalytic activity of different catalysts

Starting materials	Fe preloaded process	Reduction process	Structure	PMS/PMS catalyst	Fenton catalyst	Reference
old corrugated containers, $FeCl_3 \cdot 6H_2O$	shear mixing	carbonization	graphene oxide-like 2D biochar stabilized nZVI	30 mg/L BPA were nearly completely removed in 15 min at pH 7	30 mg/L BPA were nearly completely removed in 25 min at pH 7	This work
graphite powder, $FeSO_4 \cdot 7H_2O$	graphite powder oxidized to graphene oxide by Hummers method, graphene oxide and methanol/water were ultrasonically stirred, $FeSO_4 \cdot 7H_2O$ added	$NaBH_4$ solution was dropwise added with vigorous stirring under nitrogen atmosphere.	nZVI dispersed on the surface of graphene	persulfate activation with 92.1% of atrazine removed within 21 min.	unknown	*Chemical Eng. J. 2018,341, 126-136*
graphite powder, $NaNO_3$ H_2SO_4, $KMnO_4$, H_2O_2, $FeSO_4 \cdot 7H_2O$	graphite powder oxidized to graphene oxide by Hummers method, graphene oxide and ultrapure water were sonicated for 2 h. 3 g $FeSO_4 \cdot 7H_2O$ added	$NaBH_4$ dissolved in ultrapure water was dropwise added to the flask at 20°C for 2.5 h.	reduced graphene oxide supported nZVI	nearly complete dechlorination of TCE was obtained	nearly complete dechlorination of TCE was obtained	*J. Hazard. Mater. 2018, 349, 35-44*
Graphite flask, $FeCl_3 \cdot 6H_2O$, $FeSO_4 \cdot 7H_2O$ and $NaBH_4$	Preparation of Fe_3O_4–rGO was redispered in oxygen free water. $FeSO_4 \cdot 7H_2O$ dissolved in deionized water and then transferred to the solution	$NaBH_4$ alkaline aqueous was added	nZVI immobilized on magnetic Fe_3O_4–reduced graphene oxide	unknown	98.0% removal of 50 mg/L MB achieved within 60 min at pH 3.00	*J. Water Process Eng. 2015, 5, 101-111*
Expandable graphite, $FeSO_4 \cdot 7H_2O$ and $NaBH_4$	$FeSO_4 \cdot 7H_2O$ dissolved in 200 mL deionized water and mixed with the fresh Fe_3O_4/graphene oxide under vigorous mechanical stirring for 60 min	$NaBH_4$ was added dropwise and stirred for 60 min	Fe^0/Fe_3O_4/graphene composite	unknown	Methyl Orange (94.78%), Methylene Blue (91.60%) and Crystal Violet (89.07%) were removal in 20 min	*J. Environ. Sci. 2016, 44, 148-157*

sawdust, $FeCl_3 \cdot 6H_2O$	sawdust was added $FeCl_3 \cdot 6H_2O$ solution, the mixture was rotary evaporation, and the residue was dried at 80 °C overnight.	carbonization	nanofiber structure	20 mg/L of BPA were completely removed in 5 min	unknown	*Chemical Eng. J. 2019,359, 572-583*
rice hull, $FeSO_4 \cdot 7H_2O$	Biochars were dissolved in $FeSO_4 \cdot 7H_2O$ solution, then N_2 was purged into the solution for 1 h.	dropwise addition of 250 mL $NaBH_4$	rough and porous surface morphologies	99.4% TCE was removed within 5 min at pH 6.2	unknown	*Bioresour. Technol. 2015, 175, 269-274*
rice husk, $FeSO_4 \cdot 7H_2O$	biochar was dissolved in $FeSO_4 \cdot 7H_2O$ solution and stirred for 1 h. The solution was degassed by purging N_2 for 1 h.	$NaBH_4$ was added dropwise with vigorous stirring at room temperature.	rough and porous shape	The degradation efficiency of Nonylphenol (20 mg/L) was 96.2% within 120 min	unknown	*Chemical Eng. J. 2017, 311, 163-172*
cornstalk, $FeCl_3 \cdot 6H_2O$	biochars were soaked into $FeCl_3 \cdot 6H_2O$ solution for 24 h under room temperature.	$NaBH_4$ was added dropwise, followed by stirring for another 30 min.	nZVI/BC composites	unknown	removal efficiency (74.04%) of SMT was achieved at the optimal conditions pH 3	*Sep. Purif. Technol. 2018, 202, 130-137*
kenaf bar, $FeSO_4 \cdot 7H_2O$	biochar was mixed with $FeSO_4 \cdot 7H_2O$ to form a mixture of the biochar and iron	green tea extract was added under N_2 atmosphere	spherical particles were formed on the biochar surface	remove efficiencies of BPA could reach 98% in 60 min	unknown	*Environ. Pollut. 2018, 239, 698-705*
rice husk, $FeSO_4 \cdot 7H_2O$	biochar was dispersed in oxygen free ultrapure water. Then, 0.0135 mol $FeSO_4 \cdot 7H_2O$ was added at pH 5.0.	$NaBH_4$ was added dropwise. The solution was stirred for 2 h	ZVI was homogeneously loaded on biochar surface	unknown	efficiently activate H_2O_2 to achieve TCE degradation efficiency of 98.9% within 30 min	*Scientific Reports 2017, 7, 43051*

gasification plant, $FeSO_4·7H_2O$	biochar was dissolved in ethanol and 20 mL of 0.23 M $FeSO_4·7H_2O$ solution was added	$NaBH_4$ was added dropwise. The solution was stirred for another 20 min	nZVI were dispersed in the holes of the biochar tubes	activation of PS for 1028.02 mg/L COD could be removed within 120 min.	unknown	*Chemical Eng. J. 2019, 359, 1215-1223*
Melamine,d-glucose, $FeCl_3·6H_2O$, $FeCl_2·4H_2O$	Melamine, d-glucose, $FeCl_3·6H_2O$ and $FeCl_2·4H_2O$ were dissolved in water, followed by 1 h stirring. 28% ammonia solution was added dropwisely, and then transferred into a Teflon-lined autoclave and treated in an oven at 180 °C for 18 h.	annealed in N_2 atmosphere	regular nanospheres were formed with a diameter around 20–30 nm	activation of oxone® for phenol degradation by complete removal of 20 ppm phenol within 10 min.	unknown	*Appl. Catal., B. 2015, 172-173, 73-81.*
sugarcane residue, $FeSO_4·7H_2O$	sugarcane residue was impregnated in $FeSO_4·7H_2O$ solution and mixed for 24 h, and filtered by a vacuum suction and dried at 60 °C for 24 h.	pyrolyzed	Fe-impregnated sugarcane biochar	unknown	High removal efficiency of 99.7% was achieved within 2 h at initial pH 5.5 under 25 °C.	*Bioresour. Technol. 2018, 249, 368-376*
peanut shells, $FeSO_4·7H_2O$	5.0 g $FeSO_4·7H_2O$ and 1.0 g biochar were put in 250 mL deionized water and stirred	$NaBH_4$ solution was added dropwise and stirred vigorously	nZVI distributed on the sticks of the biochar	The removal of diatrizoate reached nearly 100% at pH 3.0 and 25 °C.	unknown	Int. J. Environ. Res. Public Health *2018, 15, 1937.*

Table s2. Properties of the as-synthesized nZVI/biochar OCF-850 and OCF-850 used.

	S_{BET}	Porosity	Pore Volume	Pore Size	Elemental percentage (%)		
	m^2/g	%	cm^3/g	nm	C	O	Fe
OCF-850	140.84	22.3	0.044	2.55	70.18	8.22	16.41
OCF-850 used	137.49	21.9	0.038	2.40	70.77	8.93	15.95

Table s3. The degradation of BPA under various conditions.

pH	PMS amount	Fe^{2+} Addition	Catalyst Addition	Rate / min^{-1}
4	40 mg	0 mg/L	0.05 g	1.299±0.024
4	40 mg	0 mg/L	0	0.131±0.022
4	40 mg	3.11 mg/L	0	0.178±0.020
7	40 mg	0 mg/L	0.05 g	0.351±0.032
7	40 mg	0 mg/L	0	0.0452±0.0013
7	40 mg	0.27 mg/L	0	0.0598±0.0054
10	40 mg	0 mg/L	0.05 g	0.316±0.029
10	40 mg	0 mg/L	0	0.0320±0.0024
10	40 mg	0.053 mg/L	0	0.0383±0.0022
pH	H_2O_2 amount	Fe^{2+} Addition	Catalyst Addition	Rate / min^{-1}
4	1 ml 3%	0 mg/L	0.05 g	1.105±0.048
4	1 ml 3%	0 mg/L	0	0.104±0.0083
4	1 ml 3%	3.42 mg/L	0	0.127±0.036
7	1 ml 3%	0 mg/L	0.05 g	0.194±0.014
7	1 ml 3%	0 mg/L	0	0.0474±0.0055
7	1 ml 3%	0.34 mg/L	0	0.0480±0.0014
10	1 ml 3%	0 mg/L	0.05 g	0.053±0.0017
10	1 ml 3%	0 mg/L	0	0.00946±0.00043
10	1 ml 3%	0.063 mg/L	0	0.00987±0.0024

Note: all of the tests were conducted in triplicate.

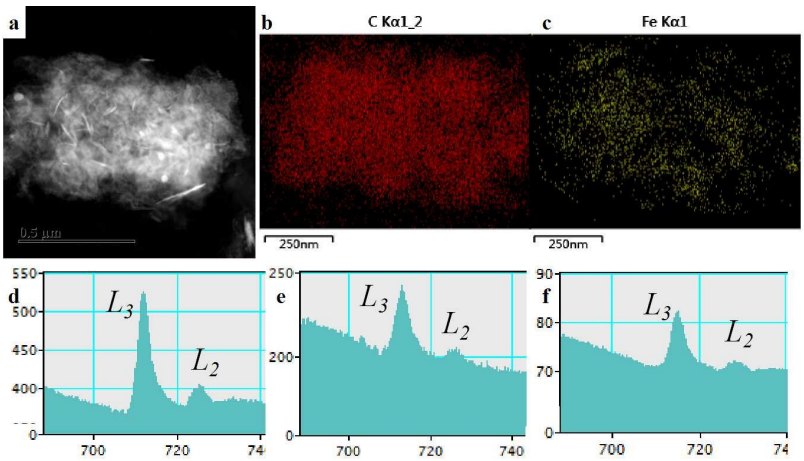

Fig. s1. STEM-EDS elemental mapping of the as-synthesized 2D nZVI/biochar OCF-850(a), (b) C, (c) Fe, and typical EELS spectra of the OCF-850 (d-f).

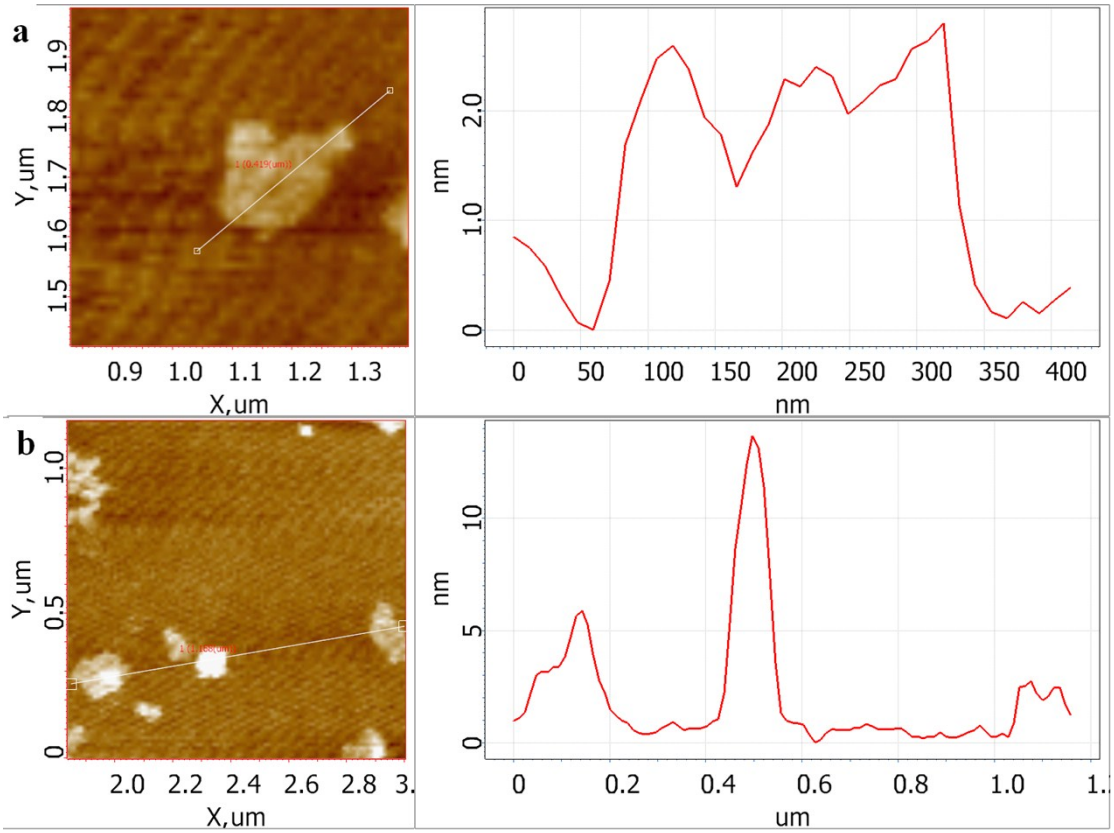

Fig. s2. Typical AFM images of the as-synthesized OCF-850 and the corresponding section analyses.

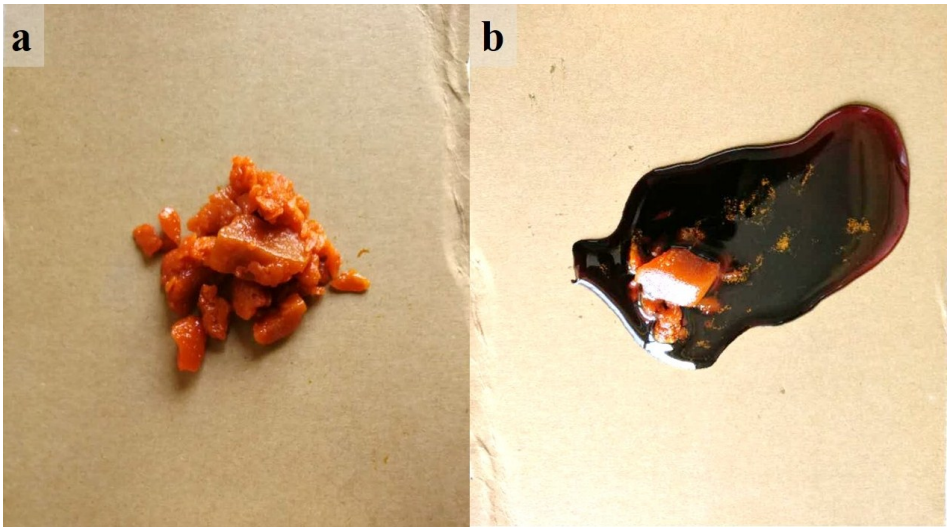

Fig. s3. Photographs of fresh $FeCl_3 \cdot 6H_2O$ stark on the surface of the OCC (a) and after exposure to the air after 1 h (b).

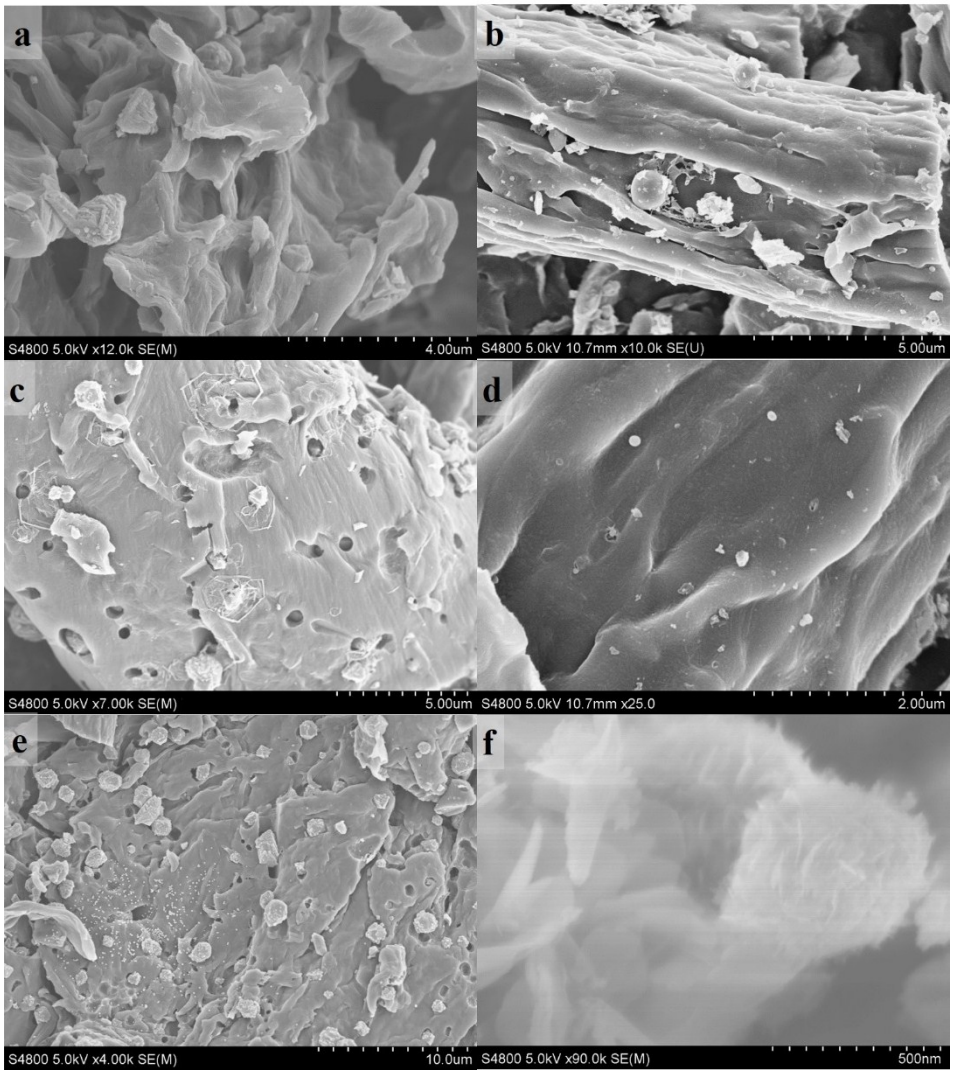

Fig. s4. SEM images of the OCC-derived materials produced under different conditions, (a) OCC-850, (b) carbonization of $FeCl_3 \cdot 6H_2O$ loaded OCC at 850 °C and then shearing 10 min; (c) carbonization of $Fe(NO_3)_3 \cdot 9H_2O$ loaded OCC at 850 °C and then shearing 10 min; (d) carbonization of $CuCl_2 \cdot 2H_2O$ loaded OCC at 850 °C and then shearing 10 min; (e) carbonization of $Fe(NO_3)_3 \cdot 9H_2O$ and $CuCl_2 \cdot 2H_2O$ loaded OCC at 850 °C and then shearing 10 min; and (f) of shearing mixing of $Fe(NO_3)_3 \cdot 9H_2O$ and $CuCl_2 \cdot 2H_2O$ loaded OCC for 10 min and then carbonization at 850 °C.

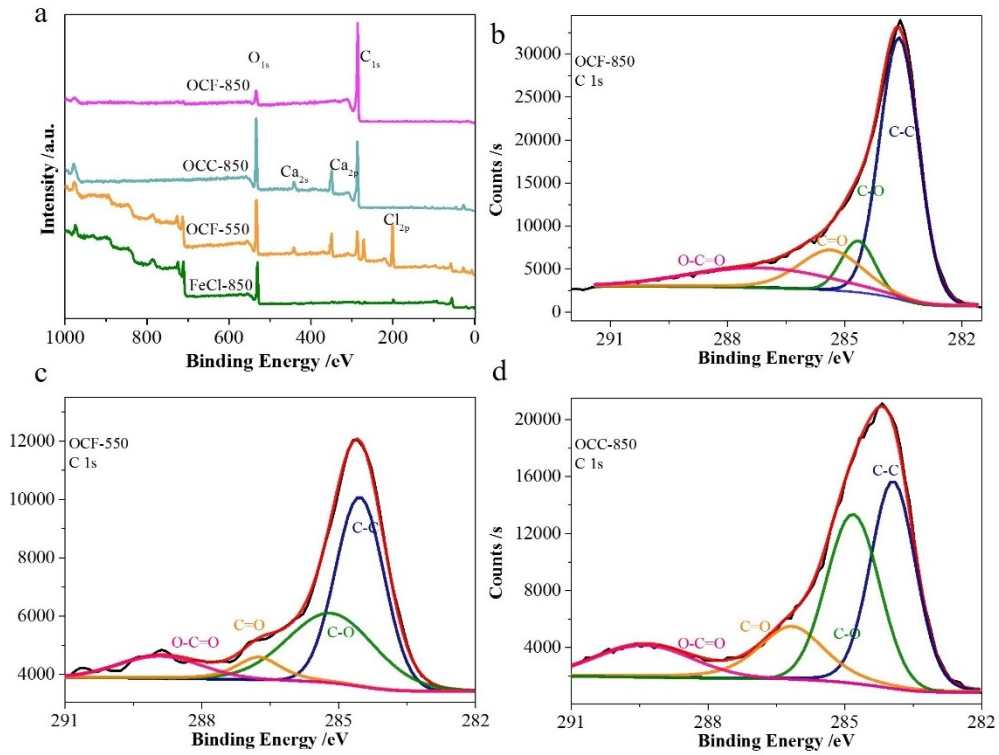

Fig. s5. XPS spectra of the as-synthesized materials (a), the high resolution C 1s spectra of OCF-850 (b), OCF-550 (c) and OCC-850 (d).

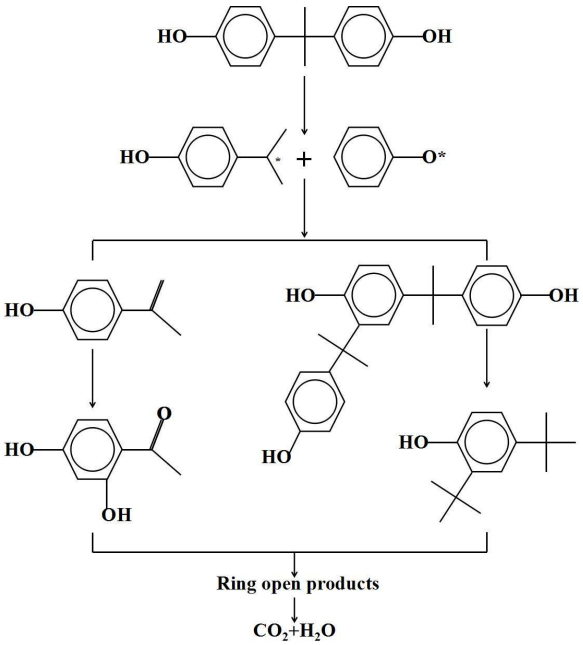

Fig. s6. Possible degradation pathway of BPA induced by the activation of PMS over OCF-850.

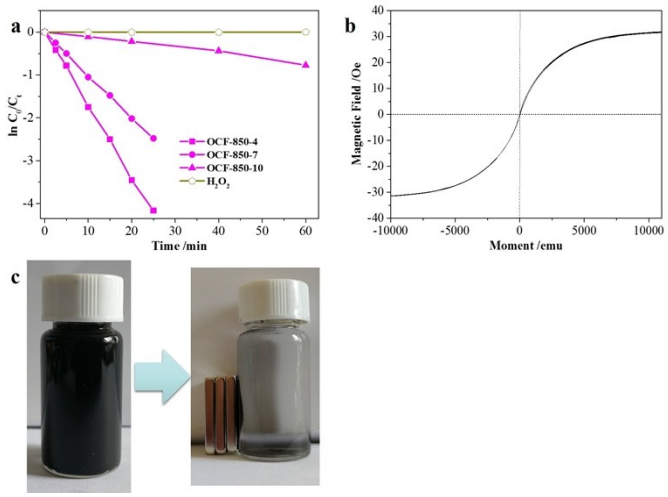

Figure s7. (a) The relative concentration profiles of BPA during typical Fenton degradation processes under dark conditions, (b) the magnetic hysteresis loop of OCF-850, and (c) the magnetic separation of the OCF-850 dispersed in a C_2H_5OH solution.

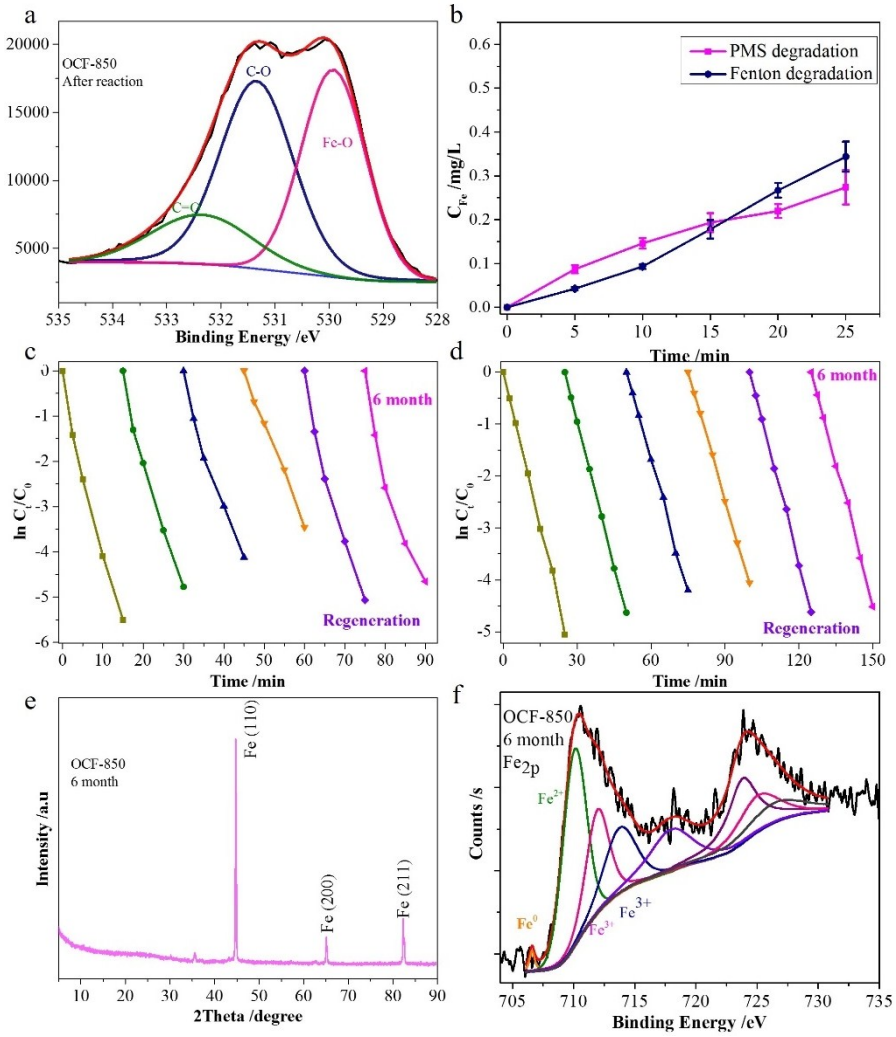

Fig. s8. The high resolution O 1s spectra of OCF-850 after typical PMS degradation process (a), Leaching of Fe ions during the degradation process (b), Cyclic degradation in repetitive degradation of BPA during typical PMS degradation processes (c), during typical Fenton degradation processes (d), the XRD spectrum of OCF-850 after 6 month (e), and the high resolution Fe2p spectra after 6 month (f).

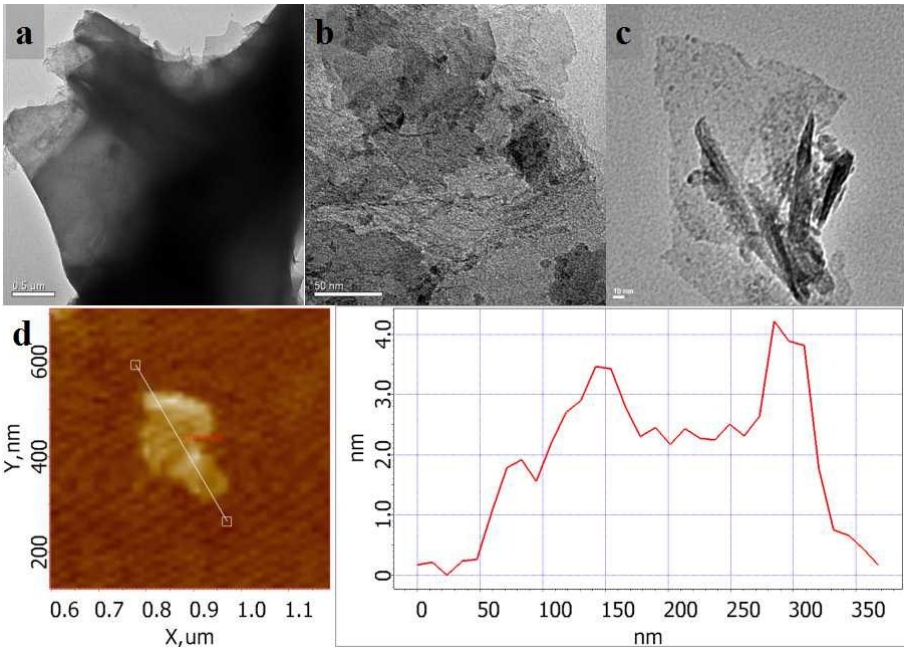

Figure s9. Typical TEM images (a-c) and AFM image (d) of the OCF-850 after the catalysis.